Elastic properties of surfactant monolayers at liquid–liquid interfaces: A molecular dynamics study

ARTICLE *in* THE JOURNAL OF CHEMICAL PHYSICS · MAY 2000

Impact Factor: 2.95 · DOI: 10.1063/1.481486

2 AUTHORS, INCLUDING:

Mohamed Laradji
The University of Memphis
99 PUBLICATIONS **1,603** CITATIONS

SEE PROFILE

Elastic properties of homopolymer-homopolymer interfaces containing diblock copolymers

Mohamed Laradji
Department of Physics, University of Prince Edward Island, Charlottetown, PEI, Canada C1A 4P3

Rashmi C. Desai
Department of Physics, University of Toronto, Toronto, Ontario, Canada M5S 1A7

(Received 10 October 1997; accepted 12 December 1997)

We study the elastic properties of homopolymer/homopolymer interfaces containing diblock copolymers by means of a theory of Gaussian fluctuations. The interfacial tension and the bending rigidity of the interface in the two-phase coexistence region are calculated from the power spectrum of capillary modes. Our theory shows that in the limiting case of a pure binary homopolymer mixture, while the interfacial tension increases monotonically with increasing χN (where χ is the Flory-Huggins parameter and N is the homopolymer molecular weight) the bending rigidity does not. The bending rigidity increases rapidly at first for small values of χN, but then decreases with further increase of χN. In the presence of diblock copolymers, the interfacial tension always decreases with increasing diblock copolymer volume fraction at a given χN. However, the bending rigidity can show either a decrease or an increase depending on χN and the ratio γ between the molecular weights of a diblock copolymer and that of a homopolymer. Our results for the surface pressure and the bending rigidity are further compared with results based on scaling arguments of wet polymer brushes. © *1998 American Institute of Physics.* [S0021-9606(98)51111-7]

I. INTRODUCTION

Homopolymer blends allow us to design new composite materials with tailored characteristics. However, due to the ultra-low entropy of mixing of the long homopolymer chains, a typical binary homopolymer blend is usually found in an immiscible state, and has consequently poor mechanical properties. New high-strength composite polymeric materials composed of pre-existing homopolymers can be built through the addition of even small amounts of block copolymers to the mixture. Since such block copolymers are typically long polymer chains formed of two blocks, each one having a preferential affinity with one of the homopolymers, they prefer to segregate at the homopolymer/homopolymer interfaces, thereby leading to a reduction of the interfacial tension. The decrease of the interfacial tension may balance the entropy of mixing leading to a disordered, microemulsion-like, phase.[1] The addition of block copolymers is also able to create ordered phases in the mixture with a variety of morphologies similar to those seen in pure block copolymer melts.

Experimental[1–7] and theoretical studies of block copolymers, [8–20] as useful compatibilizing agents, has been an active area of research for many years, driven mainly by technological applications. Our interest in studying block copolymers at interfaces is also motivated by the fact that these systems can well be regarded as a theoretical model for the more complex biological systems.

Self-consistent field theories have been successful in predicting the effect of diblock copolymers on the interfacial tension.[9–11,14] However, the effect of the diblock copolymers on the bending properties of an interface has not been thoroughly studied. Wang and Safran[17] analyzed these effects in the limit of strongly stretched diblock copolymers. More recently, Matsen and Schick[18] studied these effects using a single order-parameter Ginzburg-Landau theory, in which the coefficients of the space dependent gradient terms are derived from the coefficients of the power of the wavevector, q^n, appearing in the inverse of the scattering intensity, as determined from Leibler's theory.[21] It should be noticed, however, that Leibler's theory provides us with the scattering function of a homogeneous phase, whereas the system containing diblock copolymers, that we are considering, is inhomogeneous. The Ginzburg-Landau theory is therefore expected to be valid only in the limiting case where gradients of the volume fractions across the interface are very weak.

In the present paper, we investigate the effect of specifically diblock copolymers on both tension and bending rigidity of A-homopolymer/B-homopolymer interfaces using our recently developed self-consistent theory of anisotropic fluctuations.[22–25] Our motivation in developing this theory was to investigate the thermodynamic stability of the ordered phases in diblock copolymer melts and the kinetic pathways of order-order phase transitions, and to calculate the anisotropic scattering functions from which elastic constants were extracted. In the present paper, we formulate a theory of Gaussian fluctuations for ternary mixtures containing two immiscible homopolymers and diblock copolymers in the two-phase region, and calculate the power spectrum of the interfacial capillary modes from the two-point correlation function of the local volume fractions. The elastic constants are then extracted by analyzing the scattering functions for long wavelengths.

We find that at a given temperature, whereas the interfacial tension decreases monotonically with increasing the bulk volume fraction of diblock copolymers, the behavior of the bending rigidity is more complex. Specifically, for relatively large temperatures, increasing the amount of diblock copolymers leads to a decrease in the bending rigidity. On the other hand, for relatively low temperatures, the bending rigidity at first decreases with increasing diblock copolymer concentration for small diblock copolymer volume fractions, and then increases as the copolymer volume fraction is further increased.

The paper is organized as follows. In Sec. II, the theory of ternary mixtures of two homopolymers and diblock copolymers in the semi-grand canonical ensemble is given. This includes the theoretical model, a brief account of the self-consistent field theory followed by our theory of Gaussian anisotropic fluctuations. The results of this theory, including the limiting case of a binary homopolymer blend, are then presented in Sec. III. Finally, the last section is devoted to a summary and concluding remarks. Details of the theory and the numerical techniques are given in Appendices A and B.

II. THEORY OF TERNARY MIXTURES CONTAINING DIBLOCK COPOLYMERS

A. Model and free energy functional

The phase behavior of a ternary mixture of n_A A-homopolymers, n_B B-homopolymers and n_C AB-diblock copolymers may be studied in terms of the ''standard'' model which is based on three essential ingredients: (1) local monomer-monomer interactions, (2) incompressibility condition, and (3) fully flexible chains. We focus on the case where the polymerization indices of the two homopolymers are both equal to N and that of the diblock copolymers is equal to γN. We moreover consider symmetric diblock copolymers (i.e., number of effective monomeric segments (statistical segments) of each of the two blocks are equal to $\gamma N/2$). We find it useful to use the convention in which all lengths are rescaled by the radius of gyration of either of the homopolymers, $R_g = b(N/6)^{1/2}$ (assuming that the statistical segment lengths of the two monomer types are both equal to b); furthermore the running coordinate along the chain is rescaled by N, and is denoted by t. The semi-grand-canonical partition function of the mixture may then be written as (within an irrelevant multiplicative factor)[15]

$$\Xi = \sum_{n_A,n_B,n_c}^{\infty} \frac{\exp\{\mu_A n_A + \mu_B n_B + \mu_c n_c\}}{n_A! n_B! n_c!} \int \prod_{i=1}^{n_A} \mathscr{D}\mathbf{r}_i^{h,A} \prod_{j=1}^{n_B} \mathscr{D}\mathbf{r}_j^{h,B} \prod_{k=1}^{n_c} \mathscr{D}\mathbf{r}_k^{c} \prod_{\mathbf{r}} \delta\left[1 - \hat{\phi}_c(\mathbf{r}) - \sum_{\alpha} \hat{\phi}_\alpha(\mathbf{r})\right]$$
$$\times \mathscr{P}_A(\{\mathbf{r}^{h,A}\}) \mathscr{P}_B(\{\mathbf{r}^{h,B}\}) \mathscr{P}_c(\{\mathbf{r}^{c}\}) \exp\left\{-\frac{\rho_0 R_g^3}{N} \int d\mathbf{r} \chi N \hat{\phi}_A(\mathbf{r}) \hat{\phi}_B(\mathbf{r})\right\}, \tag{1}$$

where μ_α (with $\alpha = A, B$) is the chemical potential of homopolymer α and μ_c is the chemical potential of diblock copolymers. ρ_0 is the mixture's number density. The δ-function in Eq. (1) accounts for the incompressibility condition. The connectivity of the monomers within a chain of type α is ensured through the probability distribution, $\mathscr{P}_\alpha$, which for fully flexible chains is given by

$$\mathscr{P}_\alpha(\{\mathbf{r}^{h,\alpha}\}) = \prod_{i=1}^{n_\alpha} \exp\left[-\frac{1}{4}\int_0^1 dt \left(\frac{d\mathbf{r}_i^{h,\alpha}(t)}{dt}\right)^2\right]$$
$$\text{for } \alpha = A,B \tag{2}$$

and

$$\mathscr{P}_c(\{\mathbf{r}^{c}\}) = \prod_{i=1}^{n_c} \delta[\mathbf{r}_i^{c,A}(\gamma/2) - \mathbf{r}_i^{c,B}(\gamma/2)]$$
$$\times \prod_{\alpha} \exp\left[-\frac{1}{4}\int_0^{\gamma/2} dt \left(\frac{d\mathbf{r}_i^{c,\alpha}(t)}{dt}\right)^2\right] \tag{3}$$

for the diblock copolymers. The δ-function in Eq. (3) ensures the connectivity between the A- and B-blocks within a single copolymer chain. In Eq. (1), the volume fractions of monomers of type α is given by

$$\hat{\phi}_\alpha(\mathbf{r}) = \hat{\phi}_\alpha^h(\mathbf{r}) + \hat{\phi}_\alpha^c(\mathbf{r}), \tag{4}$$

where

$$\hat{\phi}_\alpha^h(\mathbf{r}) = \frac{N}{\rho_0 R_g^3} \sum_{i=1}^{n_\alpha} \int_0^1 dt\, \delta(\mathbf{r} - \mathbf{r}_i^{h,\alpha}(t)), \tag{5}$$

is the contribution due to the α-monomers belonging to α-homopolymers, and

$$\hat{\phi}_\alpha^c(\mathbf{r}) = \frac{N}{\rho_0 R_g^3} \sum_{i=1}^{n_c} \int_0^{\gamma/2} dt\, \delta(\mathbf{r} - \mathbf{r}_i^{c,\alpha}(t)), \tag{6}$$

is the contribution due to the α-monomers belonging to the diblock copolymers. The functional integral over the polymer conformations in Eq. (1) is then turned into a more tractable functional integral through the replacement of $\exp\{-(\rho_0 R_g^3/N)\int d\mathbf{r}\chi N \hat{\phi}_A(\mathbf{r})\hat{\phi}_B(\mathbf{r})\}$ by

$$\int \prod_{\alpha} \{\mathscr{D}\phi_\alpha(\mathbf{r})\, \delta(\phi_\alpha(\mathbf{r}) - \hat{\phi}_\alpha(\mathbf{r}))\}$$
$$\times \exp\left[-\frac{\rho_0 R_g^3}{N} \int d\mathbf{r} \chi N \phi_A(\mathbf{r}) \phi_B(\mathbf{r})\right] \tag{7}$$

in Eq. (1), where ϕ_α is the volume fraction field of the α-monomers. The delta-function in Eq. (7) can be replaced by its integral representation through the introduction of two auxiliary fields ω_A and ω_B. This yields to the following partition function for the ternary mixture system:

$$\Xi = \int \prod_{\alpha} \{\mathscr{D}\phi_\alpha \mathscr{D}\omega_\alpha\} \mathscr{D}\eta \times \exp[-\mathscr{F}(\{\phi_\alpha\},\{\omega_\alpha\},\{\eta\})], \tag{8}$$

with the free energy functional, $\mathscr{F}$, given by

$$\mathscr{F}(\{\phi_\alpha\},\{\omega_\alpha\},\{\eta\}) = \frac{\rho_0 R_g^3}{N}\Bigg\{ \int d\mathbf{r}\Bigg[\chi N \phi_{\mathrm{A}}(\mathbf{r})\phi_{\mathrm{B}}(\mathbf{r}) - \sum_\alpha \omega_\alpha(\mathbf{r})\phi_\alpha(\mathbf{r}) + \eta(\mathbf{r})\Bigg(\sum_\alpha \phi_\alpha(\mathbf{r}) - 1\Bigg)\Bigg] - \sum_\alpha e^{\mu_\alpha} z_\alpha(\{\omega_\alpha\}) - e^{\mu_c} z_c(\{\omega_{\mathrm{A}}\},\{\omega_{\mathrm{B}}\})\Bigg\}. \tag{9}$$

In the free energy functional above, the local incompressibility constraint is ensured through the local Lagrange-multiplier field η. z_α ($\alpha =$ A, B) and z_c are partition functions of single chains A, B and c, respectively, in the presence of the auxiliary fields ω_{A} and ω_{B}. The single chain partition functions can be expressed in terms of the propagator, $Q_\alpha(\mathbf{r},t|\mathbf{r}')$, which quantifies the statistical weight of finding a portion of a chain belonging to species α provided that its end monomer is located at $\mathbf{r}'$ and that the monomer at chain-coordinate t is located at $\mathbf{r}$. The single chain partition functions can therefore be written in terms of these propagators as follows:

$$z_\alpha(\{\omega_\alpha\}) = \int d\mathbf{r} d\mathbf{r}' Q_\alpha(\mathbf{r},1|\mathbf{r}'), \tag{10}$$

for the homopolymers and

$$z_c(\{\omega_{\mathrm{A}}\},\{\omega_{\mathrm{B}}\}) = \frac{1}{V}\int d\mathbf{r} d\mathbf{r}' d\mathbf{r}'' Q_{\mathrm{A}}\left(\mathbf{r},\frac{\gamma}{2}\middle|\mathbf{r}'\right) Q_{\mathrm{B}}\left(\mathbf{r}',\frac{\gamma}{2}\middle|\mathbf{r}''\right), \tag{11}$$

for the diblock copolymers (V is the system's volume). It can be shown[26] that the propagators follow a modified diffusion equation,

$$\frac{\partial Q_\alpha(\mathbf{r},t|\mathbf{r}')}{\partial t} = \nabla^2 Q_\alpha(\mathbf{r},t|\mathbf{r}') - \omega_\alpha(\mathbf{r}) Q_\alpha(\mathbf{r},t|\mathbf{r}'), \tag{12}$$

with the boundary condition $Q_\alpha(\mathbf{r},0|\mathbf{r}') = \delta(\mathbf{r}-\mathbf{r}')$.

In the present work, since we are interested in the elastic properties of a planar A-rich/B-rich interface, it is practical to consider the case where the average volume fractions of A and B homopolymers are equal. Since the statistical segment lengths of the two monomer types are assumed to be equal, the consideration above translates into taking $\mu_{\mathrm{A}} = \mu_{\mathrm{B}} = \mu_h$. In this case, it is easy to show that by making the following transformations

$$\omega_\alpha(\mathbf{r}) - \mu_h \rightarrow \omega_\alpha(\mathbf{r}), \tag{13}$$

$$\eta(\mathbf{r}) + \mu_h \rightarrow \eta(\mathbf{r}), \tag{14}$$

$$\mu_c - \gamma\mu_h \rightarrow \mu_c, \tag{15}$$

and

$$Q_\alpha(\mathbf{r},t|\mathbf{r}') e^{\mu_h t} \rightarrow Q_\alpha(\mathbf{r},t|\mathbf{r}'), \tag{16}$$

we can eliminate the chemical potential μ_h, leading to a simplified free energy functional

$$\mathscr{F}(\{\phi_\alpha\},\{\omega_\alpha\},\{\eta\}) = \frac{\rho_0 R_g^3}{N}\Bigg\{ \int d\mathbf{r}\Bigg[\chi N \phi_{\mathrm{A}}(\mathbf{r})\phi_{\mathrm{B}}(\mathbf{r}) - \sum_\alpha \omega_\alpha(\mathbf{r})\phi_\alpha(\mathbf{r}) + \eta(\mathbf{r})\Bigg(\sum_\alpha \phi_\alpha(\mathbf{r}) - 1\Bigg)\Bigg] - \sum_\alpha z_\alpha(\{\omega_\alpha\}) - e^{\mu_c} z_c(\{\omega_{\mathrm{A}}\},\{\omega_{\mathrm{B}}\})\Bigg\}. \tag{17}$$

The expression of the free energy functional, Eq. (17), together with the modified diffusion equation, Eq. (12), constitute the basis of the subsequent calculations.

B. Self-consistent field theory

The thermodynamic properties of the ternary system can be determined if the partition function, Eq. (1), is evaluated. However, since an evaluation of the integral cannot be determined exactly, approximations must be adopted. The simplest one corresponds to the saddle-point method. It amounts to replacing the functional integral by the maximum of the integrand and ignore all fluctuations around it. This leads to the following set of equations

$$\omega_{\mathrm{A}}^{(0)}(\mathbf{r}) = \chi N[\phi_{\mathrm{B}}^{h(0)}(\mathbf{r}) + \phi_{\mathrm{B}}^{c(0)}(\mathbf{r})] + \eta^{(0)}(\mathbf{r}), \tag{18}$$

$$\omega_{\mathrm{B}}^{(0)}(\mathbf{r}) = \chi N[\phi_{\mathrm{A}}^{h(0)}(\mathbf{r}) + \phi_{\mathrm{A}}^{c(0)}(\mathbf{r})] + \eta^{(0)}(\mathbf{r}), \tag{19}$$

$$\phi_{\mathrm{A}}^{h(0)}(\mathbf{r}) = \int_0^1 dt \int d\mathbf{r}_1 d\mathbf{r}_2 Q_{\mathrm{A}}^{(0)}(\mathbf{r}_1,t|\mathbf{r}) Q_{\mathrm{A}}^{(0)}(\mathbf{r},1-t|\mathbf{r}_2), \tag{20}$$

$$\phi_{\mathrm{B}}^{h(0)}(\mathbf{r}) = \int_0^1 dt \int d\mathbf{r}_1 d\mathbf{r}_2 Q_{\mathrm{B}}^{(0)}(\mathbf{r}_1,t|\mathbf{r}) Q_{\mathrm{B}}^{(0)}(\mathbf{r},1-t|\mathbf{r}_2), \tag{21}$$

$$\phi_{\mathrm{A}}^{c(0)}(\mathbf{r}) = e^{\mu_c}\int_0^{\frac{\gamma}{2}} dt \int d\mathbf{r}_1 d\mathbf{r}_2 d\mathbf{r}_3 \times Q_{\mathrm{A}}^{(0)}(\mathbf{r}_1,t|\mathbf{r}) Q_{\mathrm{A}}^{(0)}\left(\mathbf{r},\frac{\gamma}{2}-t\middle|\mathbf{r}_2\right) \times Q_{\mathrm{B}}^{(0)}\left(\mathbf{r}_2,\frac{\gamma}{2}\middle|\mathbf{r}_3\right), \tag{22}$$

$$\phi_{\mathrm{B}}^{c(0)}(\mathbf{r}) = e^{\mu_c}\int_0^{\frac{\gamma}{2}} dt \int d\mathbf{r}_1 d\mathbf{r}_2 d\mathbf{r}_3 \times Q_{\mathrm{B}}^{(0)}(\mathbf{r}_1,t|\mathbf{r}) Q_{\mathrm{B}}^{(0)}\left(\mathbf{r},\frac{\gamma}{2}-t\middle|\mathbf{r}_2\right) \times Q_{\mathrm{A}}^{(0)}\left(\mathbf{r}_2,\frac{\gamma}{2}\middle|\mathbf{r}_3\right), \tag{23}$$

and

$$\sum_\alpha [\phi_\alpha^{h(0)}(\mathbf{r}) + \phi_\alpha^{c(0)}(\mathbf{r})] = 1, \tag{24}$$

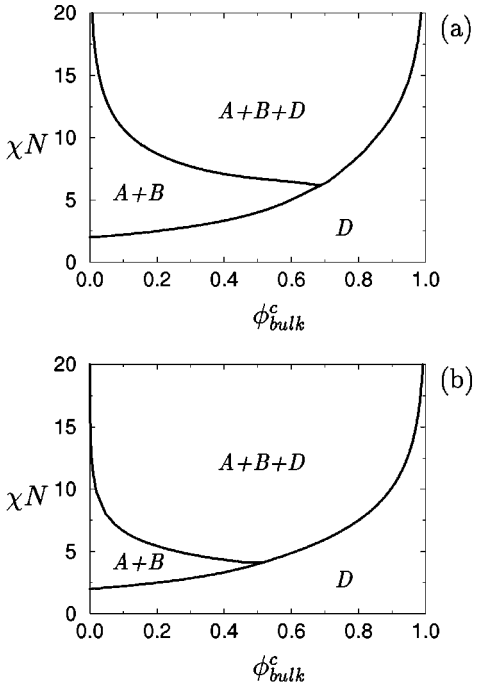

FIG. 1. Phase diagram of the three-component system for (a) $\gamma=1$ and (b) $\gamma=2$.

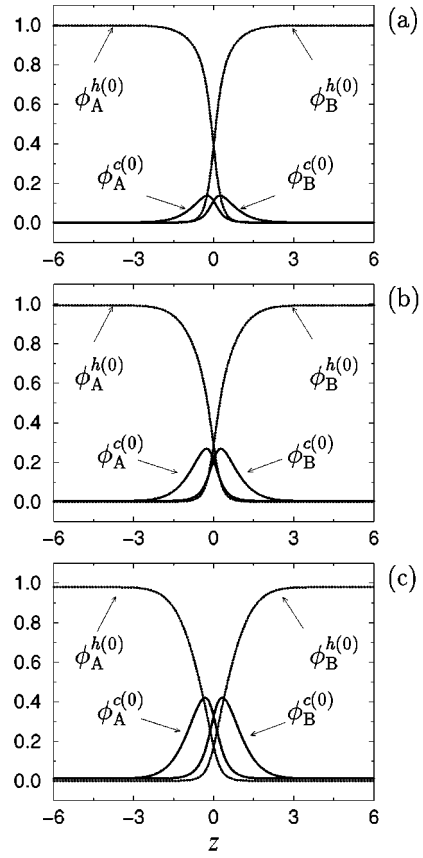

FIG. 2. Profiles, across the interface in the two-phase region, of the volume fractions, ϕ^h_A, ϕ^h_B, ϕ^c_A and ϕ^c_B for $\gamma=1$ and $\chi N=12$. (a) Corresponds to $\phi^c_{bulk}=0.252\times10^{-2}$; (b) corresponds to $\phi^c_{bulk}=0.700\times10^{-2}$; and (c) corresponds to $\phi^c_{bulk}=2.0\times10^{-2}$.

where the mean field propagators satisfy the following modified diffusion equation:

$$\frac{\partial Q^{(0)}_\alpha(\mathbf{r},t|\mathbf{r}')}{\partial t}=\nabla^2 Q^{(0)}_\alpha(\mathbf{r},t|\mathbf{r}')-\omega^{(0)}_\alpha(\mathbf{r})Q^{(0)}_\alpha(\mathbf{r},t|\mathbf{r}'), \tag{25}$$

with the boundary condition $Q^{(0)}_\alpha(\mathbf{r},t|\mathbf{r}')=\delta(\mathbf{r}-\mathbf{r}')$. It is interesting to notice from Eq. (18) to Eq. (25), that the mean field phase behavior of ternary mixtures of two homopolymers, having equal volume fractions and equal molecular weights, and diblock copolymers depends only on the combination of the three parameters $(\chi N,\mu_c,\gamma)$. The mean field phase diagram of the ternary mixture is obtained from the comparison of the free energy densities of the various phases, calculated by solving Eqs. (18) to (25) self-consistently. The detailed mean field phase diagram of this system has recently been calculated by Jannert and Schick[27] using the reciprocal space formulation of the self-consistent field theory.[28] In particular, they found that in addition to the three homogeneous A-rich, B-rich and disordered phases, the ternary mixture can also be found in a variety of periodic ordered phases similar to those seen in diblock copolymer melts.

If we neglect the fact that the ternary system can also be found in inhomogeneous periodic states, the phase diagram can be easily calculated (as shown in Appendix A). In Figs. 1(a) and 1(b), phase diagrams corresponding to $\gamma=1$ and 2 are shown, respectively. In both cases, the phase diagram exhibits the generic phase behavior of ternary systems, i.e., a two-phase coexistence region for relatively high temperatures (low χN), and a three-phase coexistence between the A-rich, B-rich and disordered phases (denoted respectively by phases A, B and D in Fig. 1) at low temperatures (high χN) and relatively large volume fractions of the diblock copolymers. Figure 1 shows that as the relative molecular weight (γ) of the diblock copolymers is increased, the tricritical point separating the consolute line from the three-phase region moves towards lower values of χN. This implies an enhancement of the ability of the diblock copolymers to mix the two homopolymers.

We have calculated the interfacial profiles, in the two-phase region of the phase diagram, by solving the self-consistent equations (18)–(25), numerically with appropriate boundary conditions. Details of numerical self-consistent field calculations are presented in Appendix B. Figure 2 displays the profiles of the volume fractions, ϕ^h_A, ϕ^h_B, ϕ^c_A and ϕ^c_B across the interface for various values of the copolymer's bulk volume fraction, ϕ^c_{bulk} for $\gamma=1$ and $\chi N=12$. [We define $\phi^c_{bulk}=\phi^{c(0)}_A(|z|\to\infty)+\phi^{c(0)}_B(|z|\to\infty)$; see also Eq. (A22).] This figure shows very clearly that the amount of accumulated copolymers at the interface is increased with increasing ϕ^c_{bulk}. The effect of increasing the relative molecular weight of the copolymers is shown through similar profiles in Fig. 3 for $\gamma=2$ but for smaller volume fractions of the copolymers, ϕ^c_{bulk}. Interestingly, this figure shows the dramatic improvement of the compatibilization effect of the diblock copolymers as their relative molecular weight γ is increased.

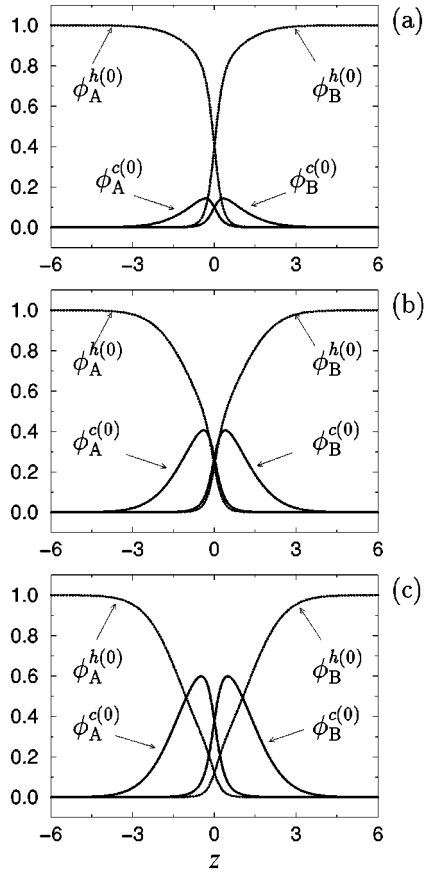

FIG. 3. Profiles of various volume fractions across the interface, in the two-phase region, for $\gamma=2$ and $\chi N=12$. (a) Corresponds to $\phi^c_{\rm bulk}=0.130\times10^{-5}$; (b) corresponds to $\phi^c_{\rm bulk}=0.961\times10^{-4}$; and (c) corresponds to $\phi^c_{\rm bulk}=0.406\times10^{-3}$.

C. Theory of Gaussian fluctuation

The interfacial tension and the bending rigidity of an interface can be calculated from the self-consistent field theory. In particular, the interfacial tension, σ, is usually calculated as the excess free energy per unit area due to the presence of a planar interface.[9–11,14,29] Using Eqs. (17), (10) and (11), its expression is given by

$$\sigma=\frac{k_BT\rho_0R_g^3}{N}\int dz\Bigg[\chi N\phi_A^{(0)}(z)\phi_B^{(0)}(z)-\sum_\alpha\ \omega_\alpha^{(0)}(z)\times\phi_\alpha^{(0)}(z)-\sum_\alpha\ q_\alpha^{(0)}(z,1)-e^{\mu_c}q_A^{c(0)}\left(z,\frac{\gamma}{2}\right)-f_{\rm bulk}\Bigg], \quad (26)$$

where $q_\alpha^{(0)}$ and $q_\alpha^{c(0)}$ are the mean field end-integrated propagators, defined in Eqs. (A1) to (A3), and $f_{\rm bulk}$ is the bulk free energy density of the A- or B-rich phase.

The bending rigidity κ can be obtained from the excess free energy of a droplet with a curved interface. In the case of a spherical droplet of radius a, for example, the excess free energy is given by

$$\Delta F=4\pi k_BT\sigma a^2+4\pi k_BT\kappa, \quad (27)$$

where we have neglected higher order dependencies on the curvature. Such approximation is only valid when a is very large. In practice, however, extracting the bending rigidity from Eq. (27) could be quite difficult to achieve since if a is large, the free energy is dominated by the interfacial tension, whereas for moderate values of a, higher order dependencies on the curvature become important.

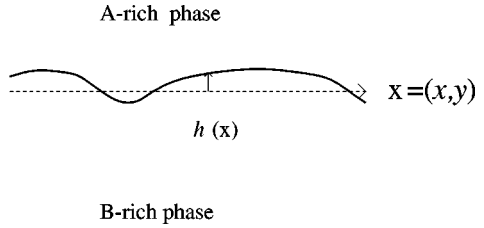

FIG. 4. Interface configuration, separating the A-rich phase from the B-rich phase at two-phase coexistence, as specified by the two-dimensional function $h(\mathbf{x})$.

The following calculations provide us with an alternative way of determining the bending rigidity without ambiguity. Instead of evaluating κ and σ from purely mean field considerations, i.e. from Eqs. (26) and (27), we can determine these constants from examining the fluctuations of the volume fractions in the two-phase region. This theory will moreover provide us with the scattering intensity of the capillary modes, a quantity which cannot be accessed from the self-consistent field theory.

In order to achieve our purpose, let us first consider an interface which fluctuates gently around its average planar position, as schematically shown in Fig. 4. We also assume that the interface does not contain overhangs. The interfacial height can then be described by a two-dimensional function $h(\mathbf{x})$ where $\mathbf{x}=(x,y)$. The long wavelength fluctuations of the interface are described by the usual capillary Hamiltonian,

$$\mathscr{H}(\{h\})=\frac{1}{k_BT}\int d\mathbf{x}\left[\frac{\sigma}{2}(\nabla_{\mathbf{x}}h)^2+\frac{\kappa}{2}(\nabla^2_{\mathbf{x}}h)^2+\cdots\right], \quad (28)$$

where $\nabla_{\mathbf{x}}=(\partial_x,\partial_y)$ is the two dimensional gradient. Neglecting the higher order terms in the expansion of Eq. (28) and using the equipartition theorem, the power spectrum of the capillary fluctuations is given by,

$$S(\mathbf{q})=\langle\tilde h_{\mathbf{q}}\tilde h_{-\mathbf{q}}\rangle=\frac{2k_BT}{\sigma q^2+\kappa q^4}, \quad (29)$$

where $\mathbf{q}=(q_x,q_y)$ and $\tilde h_{\mathbf{q}}$ is the Fourier mode of $h(\mathbf{x})$. The interfacial height fluctuations are related to the fluctuations in the difference of the volume fractions of the A and B monomers, $\psi(\mathbf{r})=\phi_A(\mathbf{r})-\phi_B(\mathbf{r})$, through the assumption that the fluctuations in the volume fraction are self-affinely distorted by $h(\mathbf{x})$, i.e.,

$$\begin{aligned}\psi(\mathbf{r})&=\psi^{(0)}(\mathbf{r})+\delta\psi(\mathbf{r})\\&\approx\psi^{(0)}(z-h(\mathbf{x}))\\&=\psi^{(0)}(z)-\frac{d\psi^{(0)}}{dz}(z)h(\mathbf{x})+\mathscr{O}(h^2).\end{aligned} \quad (30)$$

Using the Fourier modes, $\psi_{\mathbf{q}}$, of the fluctuations in the volume fraction at constant z,

$$\delta\psi(\mathbf{r}) = \frac{1}{(2\pi)^2}\int d\mathbf{x}\psi_q(z)e^{-i\mathbf{q}.\mathbf{x}}, \tag{31}$$

one finds a relationship between the Fourier mode, $\tilde{h}_{\mathbf{q}}$ and $\psi_{\mathbf{q}}(z)$,

$$\psi_{\mathbf{q}}(z) = \frac{d\psi^{(0)}}{dz}(z)h_{\mathbf{q}}. \tag{32}$$

Therefore, Eq. (32) allows us to extract the power spectrum of the capillary modes from knowledge of the scattering function of the volume fraction fluctuations. In order to achieve our goal, let us therefore expand all our fields, in the free energy functional, around their self-consistent mean field values:

$$\phi_\alpha(\mathbf{r}) = \phi_\alpha^{(0)}(\mathbf{r}) + \delta\phi_\alpha(\mathbf{r}), \tag{33}$$

$$\omega_\alpha(\mathbf{r}) = \omega_\alpha^{(0)}(\mathbf{r}) + \delta\omega_\alpha(\mathbf{r}), \tag{34}$$

$$\eta(\mathbf{r}) = \eta^{(0)}(\mathbf{r}) + \delta\eta(\mathbf{r}). \tag{35}$$

Similarly, the single chain propagators are also expanded around their mean field values,

$$Q_\alpha(\mathbf{r},t|\mathbf{r}') = Q_\alpha^{(0)}(\mathbf{r},t|\mathbf{r}') + \delta Q_\alpha(\mathbf{r},t|\mathbf{r}'). \tag{36}$$

After carrying out the expansion in terms of the fluctuating fields, one finds that the free energy functional of the system can be written as

$$\mathscr{F} = \mathscr{F}^{(0)} + \mathscr{F}^{(1)} + \mathscr{F}^{(2)} + \cdots, \tag{37}$$

where $\mathscr{F}^{(0)}$ is the mean field free energy, $\mathscr{F}^{(1)} = 0$ since the mean field solution extremizes the free energy functional, and the second order contribution is given by:

$$\begin{aligned}\mathscr{F}^{(2)}(\{\delta\phi_\alpha\},\{\delta\omega_\alpha\},\{\delta\eta\}) &= \frac{\rho_0 R_g^3}{N}\Bigg\{\int d\mathbf{r}\Bigg[\chi N\delta\phi_{\mathrm{A}}(\mathbf{r})\delta\phi_{\mathrm{B}}(\mathbf{r}) \\ &\quad - \sum_\alpha \delta\omega_\alpha(\mathbf{r})\delta\phi_\alpha(\mathbf{r}) + \delta\eta(\mathbf{r})\sum_\alpha \delta\phi_\alpha(\mathbf{r})\Bigg] \\ &\quad - \frac{1}{2}\sum_{\alpha\beta}\int d\mathbf{r}d\mathbf{r}' C_{\alpha\beta}(\mathbf{r},\mathbf{r}')\delta\omega_\alpha(\mathbf{r})\delta\omega_\alpha(\mathbf{r}')\Bigg\}.\end{aligned} \tag{38}$$

Here the two-point cumulants, $C_{\alpha\beta}(\mathbf{r},\mathbf{r}')$, are given by

$$\begin{aligned}C_{\mathrm{AA}}(\mathbf{r},\mathbf{r}') &= \int_0^1 dt_1\int_0^{t_1} dt_2 d\mathbf{r}_1 d\mathbf{r}_2[Q_{\mathrm{A}}^{(0)}(\mathbf{r}_1,1-t_1|\mathbf{r})Q_{\mathrm{A}}^{(0)}(\mathbf{r},t_1-t_2|\mathbf{r}')Q_{\mathrm{A}}^{(0)}(\mathbf{r}',t_2|\mathbf{r}_2) + Q_{\mathrm{A}}^{(0)}(\mathbf{r}_1,1-t_1|\mathbf{r}')Q_{\mathrm{A}}^{(0)}(\mathbf{r}',t_1-t_2|\mathbf{r}) \\ &\quad \times Q_{\mathrm{A}}^{(0)}(\mathbf{r},t_2|\mathbf{r}_2)] + e^{\mu_c}\int_0^{\frac{\gamma}{2}} dt_1\int_0^{t_1} dt_2\int d\mathbf{r}_1 d\mathbf{r}_2 d\mathbf{r}_3\Bigg[Q_{\mathrm{A}}^{(0)}\left(\mathbf{r}_1,\frac{\gamma}{2}-t_1\middle|\mathbf{r}\right)Q_{\mathrm{A}}^{(0)}(\mathbf{r},t_1-t_2|\mathbf{r}')Q_{\mathrm{A}}^{(0)}(\mathbf{r}',t_2|\mathbf{r}_2) \\ &\quad \times Q_{\mathrm{B}}^{(0)}\left(\mathbf{r}_2,\frac{\gamma}{2}\middle|\mathbf{r}_3\right) + Q_{\mathrm{A}}^{(0)}\left(\mathbf{r}_1,\frac{\gamma}{2}-t_1\middle|\mathbf{r}'\right)Q_{\mathrm{A}}^{(0)}(\mathbf{r}',t_1-t_2|\mathbf{r})Q_{\mathrm{A}}^{(0)}(\mathbf{r},t_2|\mathbf{r}_2)Q_{\mathrm{B}}^{(0)}\left(\mathbf{r}_2,\frac{\gamma}{2}\middle|\mathbf{r}_3\right)\Bigg],\end{aligned} \tag{39}$$

$$C_{\mathrm{AB}}(\mathbf{r},\mathbf{r}') = e^{\mu_c}\int_0\frac{\gamma}{2}dt_1\int_0\frac{\gamma}{2}dt_2\int d\mathbf{r}_1 d\mathbf{r}_2 d\mathbf{r}_3 Q_{\mathrm{A}}^{(0)}\left(\mathbf{r}_1,\frac{\gamma}{2}-t_1\middle|\mathbf{r}\right)Q_{\mathrm{A}}^{(0)}(\mathbf{r},t_1|\mathbf{r}_2)Q_{\mathrm{B}}^{(0)}\left(\mathbf{r}_2,\frac{\gamma}{2}-t_2\middle|\mathbf{r}'\right)Q_{\mathrm{B}}^{(0)}(\mathbf{r}',t_2|\mathbf{r}_3). \tag{40}$$

Similar expressions for $C_{\mathrm{BB}}(\mathbf{r},\mathbf{r}')$ and $C_{\mathrm{BA}}(\mathbf{r},\mathbf{r}')$ can be obtained by interchanging A and B in the above two equations. In the Gaussian free energy functional, $\mathscr{F}^{(2)}$, $\delta\eta(\mathbf{r})$ can be eliminated by explicitly enforcing the incompressibility constraint, i.e. letting $\Sigma_\alpha\delta\phi_\alpha(\mathbf{r}) = 0$. The incompressibility condition leads therefore to three independent fluctuating fields. We choose the following three independent combinations:

$$\delta\psi(\mathbf{r}) = \delta\phi_{\mathrm{A}}(\mathbf{r}) - \delta\phi_{\mathrm{B}}(\mathbf{r}), \tag{41}$$

$$\delta\omega(\mathbf{r}) = \frac{1}{2i}[\delta\omega_{\mathrm{A}}(\mathbf{r}) + \delta\omega_{\mathrm{B}}(\mathbf{r})], \tag{42}$$

$$\delta\zeta(\mathbf{r}) = \frac{1}{2i}[\delta\omega_{\mathrm{A}}(\mathbf{r}) - \delta\omega_{\mathrm{B}}(\mathbf{r})], \tag{43}$$

in terms of which the Gaussian free energy functional can be rewritten as

$$\begin{aligned}\mathscr{F}^{(2)}(\{\delta\psi\},\{\delta\omega\},\{\delta\zeta\}) &= \frac{\rho_0 R_g^3}{2N}\int d\mathbf{r}d\mathbf{r}'\Bigg[-\frac{\chi N}{2}\delta\psi(\mathbf{r})\delta(\mathbf{r}-\mathbf{r}')\delta\psi(\mathbf{r}') \\ &\quad - i\delta\psi(\mathbf{r})\delta(\mathbf{r}-\mathbf{r}')\delta\zeta(\mathbf{r}') - i\delta\zeta(\mathbf{r})\delta(\mathbf{r}-\mathbf{r}')\delta\psi(\mathbf{r}') \\ &\quad + \delta\zeta(\mathbf{r})C(\mathbf{r},\mathbf{r}')\delta\zeta(\mathbf{r}') + 2\delta\zeta(\mathbf{r})\Delta(\mathbf{r},\mathbf{r}')\delta\omega(\mathbf{r}') \\ &\quad + \delta\omega(\mathbf{r})\Sigma(\mathbf{r},\mathbf{r}')\delta\omega(\mathbf{r}')\Bigg],\end{aligned} \tag{44}$$

where the new two-point cumulants are given by

$$\begin{aligned}C(\mathbf{r},\mathbf{r}') &= C_{\mathrm{AA}}(\mathbf{r},\mathbf{r}') - C_{\mathrm{AB}}(\mathbf{r},\mathbf{r}') - C_{\mathrm{BA}}(\mathbf{r},\mathbf{r}') \\ &\quad + C_{\mathrm{BB}}(\mathbf{r},\mathbf{r}'),\end{aligned} \tag{45}$$

$$\begin{aligned}\Delta(\mathbf{r},\mathbf{r}') &= C_{\mathrm{AA}}(\mathbf{r},\mathbf{r}') + C_{\mathrm{AB}}(\mathbf{r},\mathbf{r}') - C_{\mathrm{BA}}(\mathbf{r},\mathbf{r}') \\ &\quad - C_{\mathrm{BB}}(\mathbf{r},\mathbf{r}'),\end{aligned} \tag{46}$$

$$\Sigma(\mathbf{r},\mathbf{r}')=C_{\mathrm{AA}}(\mathbf{r},\mathbf{r}')+C_{\mathrm{AB}}(\mathbf{r},\mathbf{r}')+C_{\mathrm{BA}}(\mathbf{r},\mathbf{r}')+C_{\mathrm{BB}}(\mathbf{r},\mathbf{r}'). \tag{47}$$

Since in the mean field theory, the inhomogeneity in our system is along the z-direction only, it is useful to project the two-point cumulants onto plane waves:

$$C^{\alpha\beta}_{\mathbf{q},\mathbf{q}'}(z,z')=\frac{1}{(2\pi)^4}\int d\mathbf{x}d\mathbf{x}'e^{-i\mathbf{q}\cdot\mathbf{x}}C_{\alpha\beta}(\mathbf{r},\mathbf{r}')e^{i\mathbf{q}'\cdot\mathbf{x}'}. \tag{48}$$

The mean field propagators can be factorized into a homogeneous part along the (x,y) plane and an inhomogeneous part along the z-axis:

$$Q^{(0)}_{\alpha}(\mathbf{r},t|\mathbf{r}')=H^{(0)}(\mathbf{x},t|\mathbf{x}')F^{(0)}(z,t|z'), \tag{49}$$

where the homogeneous part, which is solution of the free diffusion equation, is given by

$$H^{(0)}(\mathbf{x},t|\mathbf{x}')=\frac{1}{4\pi t}\exp\left[-\frac{(\mathbf{x}-\mathbf{x}')^2}{4t}\right]. \tag{50}$$

We can now calculate the Fourier components, Eq. (48), of the two point cumulants using Eqs. (49) and (50) for the propagators, and find that they are in fact diagonal in $\mathbf{q}$-space,

$$C^{\alpha\beta}_{\mathbf{q},\mathbf{q}'}(z,z')=\delta(\mathbf{q}-\mathbf{q}')C^{\alpha\beta}_{\mathbf{q}}(z,z'), \tag{51}$$

where $C^{\alpha\beta}_{\mathbf{q}}(z,z')$ are given by

$$C^{\mathrm{AA}}_{\mathbf{q}}(z,z')=\frac{1}{(2\pi)^2}\Bigg\{\int_0^1 dt_1\int_0^{t_1}dt_2e^{-(t_1-t_2)\mathbf{q}^2}\int dz_1dz_2[F^{(0)}_{\mathrm{A}}(z_1,1-t_1|z)F^{(0)}_{\mathrm{A}}(z,t_1-t_2|z')F^{(0)}_{\mathrm{A}}(z',t_2|z_2)$$
$$+F^{(0)}_{\mathrm{A}}(z_1,1-t_1|z')F^{(0)}_{\mathrm{A}}(z',t_1-t_2|z)F^{(0)}_{\mathrm{A}}(z,t_2|z_2)]+e^{\mu_c}\int_0^{\frac{\gamma}{2}}dt_1\int_0^{t_1}dt_2e^{-(t_1-t_2)\mathbf{q}^2}$$
$$\times\int dz_1dz_2dz_3\Bigg[F^{(0)}_{\mathrm{A}}\left(z_1,\frac{\gamma}{2}-t_1\middle|z\right)F^{(0)}_{\mathrm{A}}(z,t_1-t_2|z')F^{(0)}_{\mathrm{A}}(z',t_2|z_2)F^{(0)}_{\mathrm{B}}\left(z_2,\frac{\gamma}{2}\middle|z_3\right)$$
$$+F^{(0)}_{\mathrm{A}}\left(z_1,\frac{\gamma}{2}-t_1\middle|z'\right)F^{(0)}_{\mathrm{A}}(z',t_1-t_2|z)F^{(0)}_{\mathrm{A}}(z,t_2|z_2)F^{(0)}_{\mathrm{B}}\left(z_2,\frac{\gamma}{2}\middle|z_3\right)\Bigg]\Bigg\}, \tag{52}$$

$$C^{\mathrm{AB}}_{\mathbf{q}}(z,z')=\frac{e^{\mu_c}}{(2\pi)^2}\int_0^{\frac{\gamma}{2}}dt_1\int_0^{\frac{\gamma}{2}}dt_2e^{-\left(t_1+\frac{\gamma}{2}-t_2\right)\mathbf{q}^2}$$
$$\times\int dz_1dz_2dz_3\times F^{(0)}_{\mathrm{A}}\left(z_1,\frac{\gamma}{2}-t_1\middle|z\right)F^{(0)}_{\mathrm{A}}(z,t_1|z_2)F^{(0)}_{\mathrm{B}}\left(z_2,\frac{\gamma}{2}-t_2\middle|z'\right)F^{(0)}_{\mathrm{B}}(z',t_2|z_3). \tag{53}$$

Similar expressions for $C^{\mathrm{BB}}_{\mathbf{q}}(z,z')$ and $C^{\mathrm{BA}}_{\mathbf{q}}(z,z')$ can be obtained by interchanging A and B in the above two equations. The fields $\omega_{\mathbf{q}}(z)$ and $\zeta_{\mathbf{q}}(z)$ can be easily integrated out in the partition function, leading to the following quadratic free energy functional in terms of $\psi_{\mathbf{q}}(z)$,

$$\mathscr{F}^{(2)}(\{\psi_{\mathbf{q}}\})=\int d\mathbf{q}\int dzdz'\psi_{-\mathbf{q}}(z)\times[\overline{C}_{\mathbf{q}}]^{-1}(z,z')\psi_{\mathbf{q}}(z'), \tag{54}$$

where the two-point correlation matrix, $\overline{\mathbf{C}}_{\mathbf{q}}$, is given by

$$\overline{\mathbf{C}}_{\mathbf{q}}=\frac{2N}{\rho_0R_g^3}\widetilde{\mathbf{C}}^{-1}_{\mathbf{q}}\cdot\left(\mathbf{I}-\frac{\chi N}{2}\widetilde{\mathbf{C}}_{\mathbf{q}}\right). \tag{55}$$

Here $\mathbf{I}$ is the identity matrix and $\widetilde{\mathbf{C}}_{\mathbf{q}}=\mathbf{C}_{\mathbf{q}}-\mathbf{\Delta}_{\mathbf{q}}\cdot\mathbf{\Sigma}_{\mathbf{q}}\cdot\mathbf{\Delta}^T_{\mathbf{q}}$. Now, using the relationship between $\psi_{\mathbf{q}}(z)$ and $\widetilde{h}_{\mathbf{q}}$ in Eq. (32), the Gaussian free energy functional can be rewritten as:

$$\mathscr{F}^{(2)}(\{h_{\mathbf{q}}\})=\frac{\rho_0R_g^3}{2N}\int d\mathbf{q}S^{-1}(\mathbf{q})\widetilde{h}_{\mathbf{q}}\widetilde{h}_{-\mathbf{q}}, \tag{56}$$

where the capillary power spectrum is given by

$$S^{-1}(\mathbf{q})=\int dzdz'\frac{d\psi^{(0)}}{dz}(z)\frac{d\psi^{(0)}}{dz}(z')[\overline{C}_{\mathbf{q}}]^{-1}(z,z'). \tag{57}$$

For long wavelengths, the inverse of the power spectrum, $S^{-1}(\mathbf{q})$ can be expanded in powers of $\mathbf{q}$,

$$S^{-1}(\mathbf{q})=\frac{1}{2k_{\mathrm{B}}T}[\sigma R_g^2q^2+\kappa R_g^4q^4+\cdots]=\frac{1}{2}(\widetilde{\sigma}q^2+\widetilde{\kappa}q^4+\cdots), \tag{58}$$

where it can easily be shown that the scaled interfacial tension is $\widetilde{\sigma}=(N\sigma)/(k_{\mathrm{B}}T\rho_0R_g)$ and the scaled bending rigidity is $\widetilde{\kappa}=(N\kappa)/(k_{\mathrm{B}}T\rho_0R_g^3)$, with σ and κ the ''unscaled'' interfacial tension and the ''unscaled'' bending rigidity, respectively.

The numerical procedure for calculating the elastic constants of a homopolymer/homopolymer interface containing diblock copolymers is as follows:

(1) The mean field solution is determined, by numerically solving Eqs. (18) to (25) at a given point inside the two-

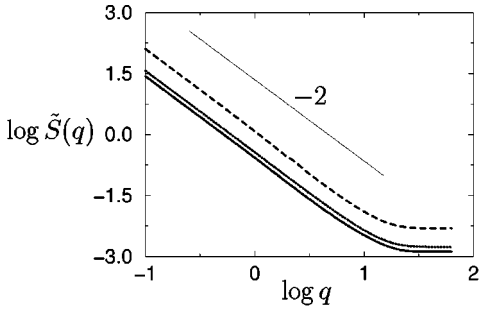

FIG. 5. Log-log plot of the power spectrum, $S(q)$ vs q for the binary homopolymer blend interface. The dashed line corresponds to $\chi N=4$, the dotted line corresponds to $\chi N=12$ and the solid line corresponds to $\chi N=20$. The slope of the thin solid line is -2.

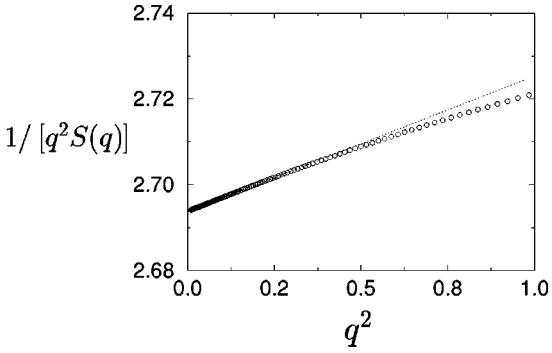

FIG. 6. $1/q^2S(q)$ vs q^2 for the binary homopolymer blend at $\chi N=12$ at long wavelengths.

phase region of the phase diagram. Examples of the profiles which we calculated are shown in Figs. 2 and 3. The self-consistent field solution provides us with the potentials $\omega^{(0)}(z)$ which are necessary for the forthcoming fluctuation calculations.

(2) The modified diffusion equations, Eq. (25), are solved using the mean field potentials obtained in **(1)**.

(3) The matrix elements of $C_{\mathbf{q}}^{\alpha\beta}(z,z')$ are constructed using Eqs. (52), (53), from which the stability matrix $\overline{\mathbf{C}}_{\mathbf{q}}$, Eq. (55), is constructed. The scattering function of the capillary modes is then calculated according to Eq. (57).

(4) The interfacial tension and the bending rigidity are then calculated respectively from the intercept and slope of $1/[q^2S(q)]$ vs q^2 at long wavelengths.

III. RESULTS

A. Binary homopolymer interface

In this subsection, we will present results for the power spectrum of the capillary waves and elastic constants in the limiting case of zero volume fraction of diblock copolymers. The interfacial power spectra, as calculated from Eq. (57), for $\chi N=4$, 12 and 20 are displayed in Fig. 5. This figure shows clearly the usual behavior of the power spectrum of a simple interface, i.e., $S(q)\sim q^{-2}$ over a wide range of wavevectors, with the proportionality constant being the inverse of the interfacial tension. However, a careful analysis of the slope at small wavelengths of $\log S(q)$ vs $\log q$ leads to an exponent which is slightly larger than -2, and which increases with increasing $\log q$. Such behavior implies that there are higher order contributions in the expansion of $\log S(q)$; the next important contribution being the bending term. Maybe the best way through which the bending rigidity is accessed is by plotting $1/[q^2S(q)]$ as a function q^2, as shown in Fig. 6 for $\chi N=12$. In this manner, the interfacial tension corresponds to the value of $1/[q^2S(q)]$ at $q=0$, whereas the bending rigidity is the slope of the function vs q^2 at very small wavevectors. It is very important to notice the deviation of $1/[q^2S(q)]$ from the linear behavior starting from small wavevectors even in the pure binary homopolymer blend. This behavior of the scattering function implies that if the bending rigidity is extracted from Eq. (27), the result should be taken with great caution due to the presence of higher order terms in the expansion.

In Fig. 7, the interfacial tension and the bending rigidity for a homopolymer/homopolymer interface are shown as a function of χN. First, Fig. 7(a) shows the expected behavior of the interfacial tension, i.e., a monotonic increase with increasing χN [see Fig. 7(a)]. However, Fig. 7(b) shows the remarkable nonmonotonic behavior of the bending rigidity as a function of χN; namely a rapid increase up to about $\chi N=5.5$, followed by a slow decrease as a function of χN. The nonmonotonic behavior of the bending rigidity can be explained as follows. In the limiting case of infinitely large molecular weights, $N\to\infty$, Helfand and Tagami,[30] using a self-consistent field calculation, have shown that the interfacial tension is actually independent of N and is given by

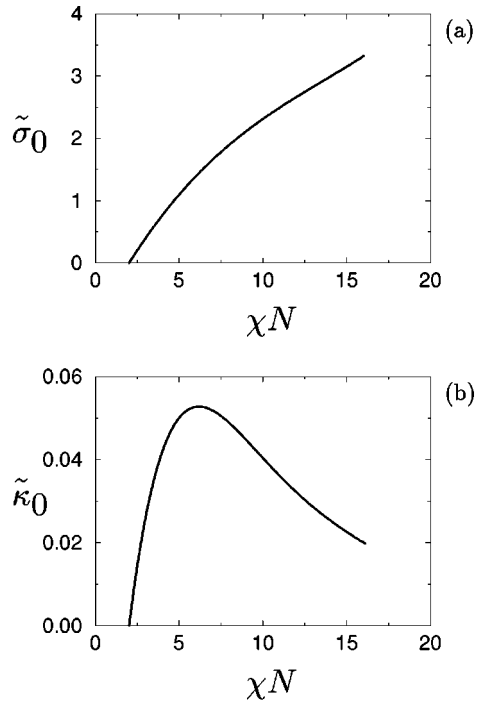

FIG. 7. (a) The interfacial tension and (b) the bending rigidity as a function of χN for the binary homopolymer blend.

$$\sigma_0 = k_B T \rho_0 b (\chi/6)^{1/2}. \tag{59}$$

In our scaled units, this translates into $\tilde{\sigma}_0 = (\chi N)^{1/2}$. They also found that the profile of the volume fraction is parabolic,

$$\phi_A^h(z) = \frac{1}{2}[1 + \tanh((\chi N)^{1/2} z)], \tag{60}$$

from which the interfacial width (in our scaled units) is derived,

$$\tilde{w}_0 = 2(\chi N)^{-1/2}. \tag{61}$$

The qualitative behavior of the bending rigidity at large molecular weights can be derived from scaling arguments and the results of Helfand and Tagami; namely, the bending rigidity has a dimension of energy, whereas the interfacial tension has the dimension of energy per unit area. Therefore based on dimensional considerations, one can write $\kappa_0 \sim \sigma_0 \tilde{w}_0^2 R_g^2$, where the presence of R_g results from the fact that w_0 is a dimensionless quantity. After the insertion of the scaling relations for w_0 and σ_0, we find $\kappa_0 \sim \chi^{-1}$, i.e. the bending rigidity decreases with increasing χ. In our scaled units, this translates into

$$\tilde{\kappa}_0 \sim (\chi N)^{-1/2} \text{ as } \chi N \to \infty. \tag{62}$$

The result of Eq. (62) implies that the bending rigidity decreases with increasing χN for large values of χN. However, since the bending rigidity must vanish at the critical point, $(\chi N)_c = 2$, we conclude that the bending rigidity of the pure binary homopolymer blend must exhibit a peak at a finite value of χN. This argument is in complete agreement with Fig. 7(b).

It is important to understand that this non-monotonic behavior of the bending rigidity is particular to polymeric systems and not generic to all binary fluids, since the mean field treatment of the ϕ^4 Ginzburg-Landau model for simple binary fluids predicts a rather vanishing bending rigidity at all temperatures, although a tiny bending rigidity may result from non-mean-field effects through a renormalization-group treatment. The presence of a finite, though very small, bending rigidity in binary homopolymer blends, even at the level of Gaussian fluctuations is the result of the nonlocal nature of the effective free energy functional which describes these systems.

B. Ternary mixtures containing diblock copolymers

We now turn our attention to the case where diblock copolymers are present. The power spectra of the capillary modes, for various values of the bulk copolymer's volume fraction, ϕ_{bulk}^c and copolymer's relative molecular weight γ, are shown in Fig. 8. While the behavior of the power spectrum is similar to that of the two-component blend for very small copolymers volume fractions or/and small values of γ, we find that as ϕ_{bulk}^c is increased or/and γ is increased, $\log S(q)$ vs q^2 starts to exhibit nonlinear behavior even at small wavevectors, signaling that the bending contribution is becoming more important as a result of the accumulation of diblock copolymers at the interface. The interfacial tension and the bending rigidity, as extracted from the behavior of

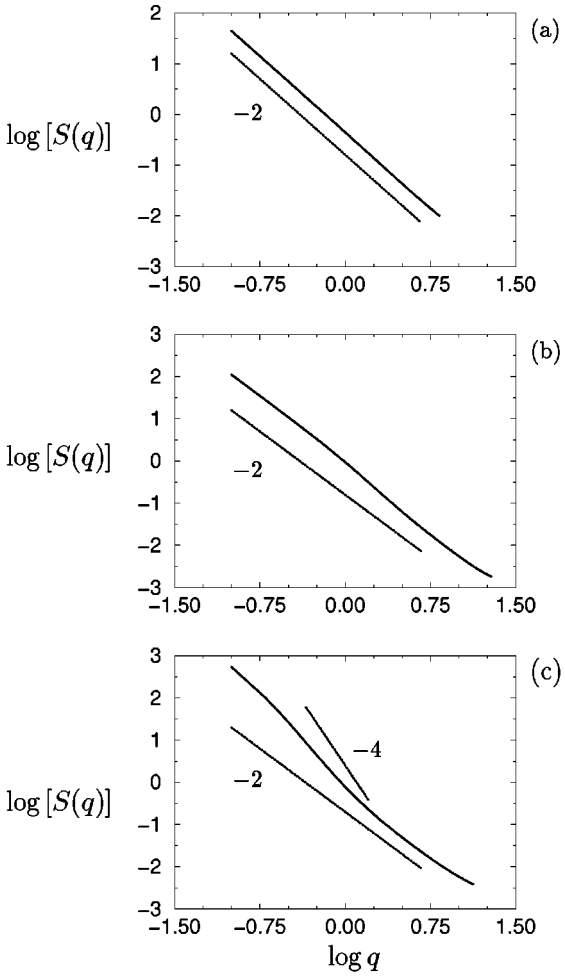

FIG. 8. Log-log plot of the height power spectrum for (a) $\gamma=1$, $\chi N=12$ and $\phi_{\text{bulk}}^c = 0.252\times10^{-2}$; compare Fig. 2(a); (b) $\gamma=1$, $\chi N=12$ and $\phi_{\text{bulk}}^c = 2.0\times10^{-2}$; compare Fig. 2(c); and (c) $\gamma=2$, $\chi N=12$ and $\phi_{\text{bulk}}^c = 0.50\times10^{-3}$; compare Fig. 3(c).

$1/[q^2 S(q)]$ vs q^2 at long wavelengths, as a function of ϕ_{bulk}^c are shown in Figs. 9–11 for various values of χN and γ. The main important effect of adding diblock copolymers to the binary homopolymer blend is the reduction of the interfacial tension. There are two sources of this reduction: (1) At high temperatures (small χN), diblock copolymers are soluble in either of the homopolymer-rich phases. This tends to decrease the value of the bulk volume fraction, and therefore to a smaller value for the interfacial tension. (2) At relatively low temperatures, the diblock copolymers are highly insoluble in the bulk, and they strongly segregate at the interface where they form a brush (see Figs. 2 and 3). In this case, the reduction of the interfacial tension is due to the positive surface pressure created by the dense copolymer layer at the interface.

In all cases (see Figs. 9(a), 10(a) and 11(a)) we find that the interfacial tension decreases with increasing the bulk copolymer volume fraction. In the particular case, where the transition from the two-phase region to the disordered phase is continuous, as in Fig. 9, the interfacial tension vanishes at the consolute line. The bending rigidity, however, does not have a unique trend as a function of ϕ_{bulk}^c. In fact, when the

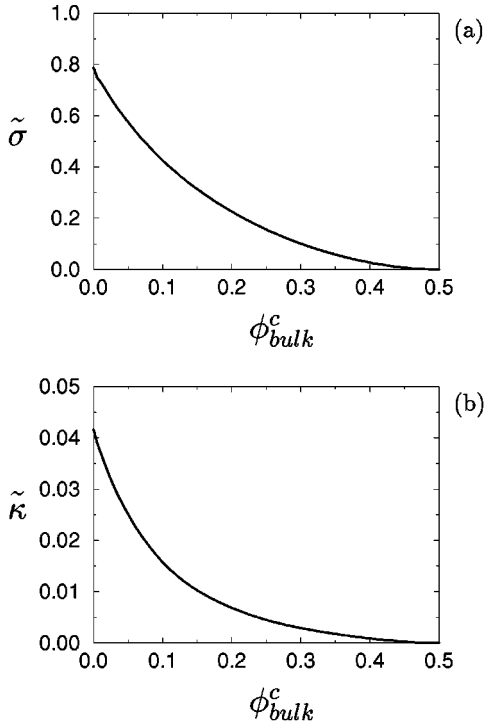

FIG. 9. (a) Surface tension and (b) bending rigidity vs the copolymer bulk volume fraction for $\gamma=1$ and $\chi N=4$.

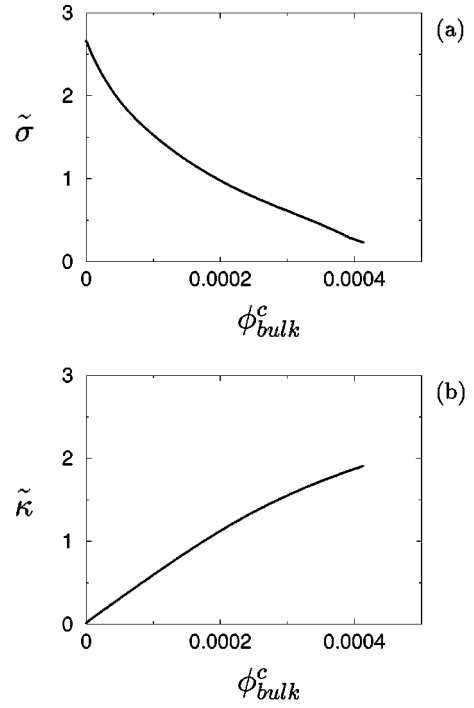

FIG. 11. Same as in Fig. 9, but for $\gamma=2$ and $\chi N=12$. Note the different scales for bending rigidity and for ϕ^c_{bulk} in Figs. 9, 10, and 11.

transition from the two-phase region to the disordered phase is continuous, we find that the bending rigidity decreases as the consolute line is approached. Indeed, the bending rigidity must vanish at the consolute line. However, for high values of χN, we find that the bending rigidity increases with increasing ϕ^c_{bulk} as shown in Figs. 10(b) and 11(b). The bending rigidity might show, however, a slight decrease from the value of the bare interface in the case of very small copolymers volume fractions and small γ. The fact that the bending rigidity decreases with increasing ϕ^c_{bulk} for relatively small χN might explain the decrease of the bending rigidity of lipid membranes on which homopolymers are adsorbed. In fact, the copolymers instead of forming a brush at the interface, are rather coiled up forming a layer similar to an adsorbed homopolymer layer on a membrane. In the adsorption case, various studies have shown that when the amount of adsorbed polymer per unit area is increased, the bending rigidity is decreased.

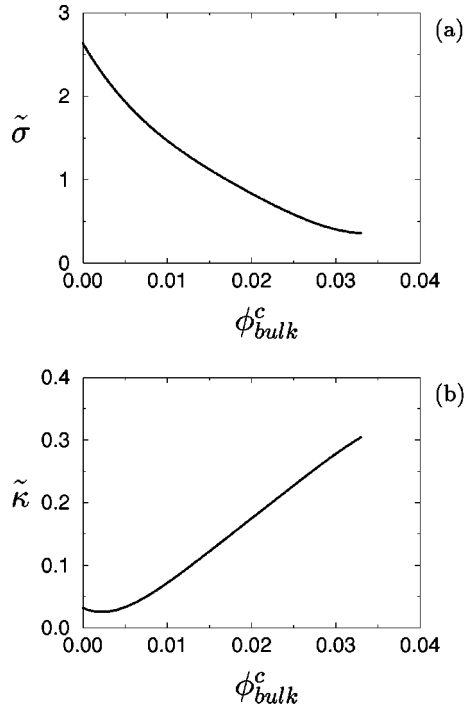

FIG. 10. Same as Fig. 9, but for $\gamma=1$ and $\chi N=12$.

We now focus on a qualitative comparison between our results and the scaling arguments presented earlier by Leibler.[13] In his analysis, the diblock copolymer layer is approximated by a polymer brush whose energy is essentially entropic (elastic entropy plus mixing entropy plus two-dimensional translational entropy). Moreover, the model ignores volume fraction gradients at the interface. When the A-homopolymers penetrate the A-block region of the copolymer brush, Leibler found that the decrease in the interfacial tension (i.e. surface pressure) is

$$(\sigma_0-\sigma)\sim c^{5/3}N^{1/3}, \tag{63}$$

where σ_0 is the interfacial tension of the bare surface and c is the surface coverage of the copolymers at the interface [$c=Q/A$ where Q is the number of diblock copolymers and A is the interfacial area]. He also found that the width of the copolymer layer is

$$w\sim c^{1/3}N^{2/3}. \tag{64}$$

Finally since the excess bending rigidity has the dimension of energy, using dimensional considerations $(\tilde{\kappa}-\tilde{\kappa}_0)\sim(\sigma_0-\sigma)w^2$, from which we find that,

$$(\kappa-\kappa_0)\sim c^{7/3}N^{5/3}, \tag{65}$$

where κ_0 is the bending rigidity of the bare homopolymer/homopolymer interface. In our scaled formalism, a direct comparison of our results with the scaling results above is not possible. However, we have direct access to the excess amount of copolymers at the interface which is defined as,

$$\Phi_{\text{excess}}=\int dz[\phi^{c(0)}(z)-\phi^c_{\text{bulk}}]. \tag{66}$$

It is easy to show that the surface coverage is related to the excess copolymer layer through the equation,

$$c=R_g\rho_0\Phi_{\text{excess}}. \tag{67}$$

Using this relationship and the scaling relations, Eqs. (63)–(65), we find the following scaling relations for the scaled interfacial tension, width and excess of bending rigidity,

$$(\tilde{\sigma}_0-\tilde{\sigma})\sim\Phi^{\alpha}_{\text{excess}}, \tag{68}$$

with $\alpha=5/3$. The width of the copolymer layer

$$\tilde{w}\sim\Phi^{\delta}_{\text{excess}}, \tag{69}$$

with $\delta=1/3$. The excess in the bending rigidity,

$$(\tilde{\kappa}-\tilde{\kappa}_0)\sim\Phi^{\beta}_{\text{excess}}, \tag{70}$$

with $\beta=7/3$. In Fig. 12, the surface pressure, width and the excess bending rigidity are plotted as a function of Φ_{excess} for various parameter values of the systems. The figure shows that the three quantities approach the scaling behavior as the triple line is approached. This is particularly true for the interfacial tension and the copolymer layer width. The asymptotic agreement between our results and the scaling results seems also to improve as the relative copolymer molecular weight, γ, is increased.

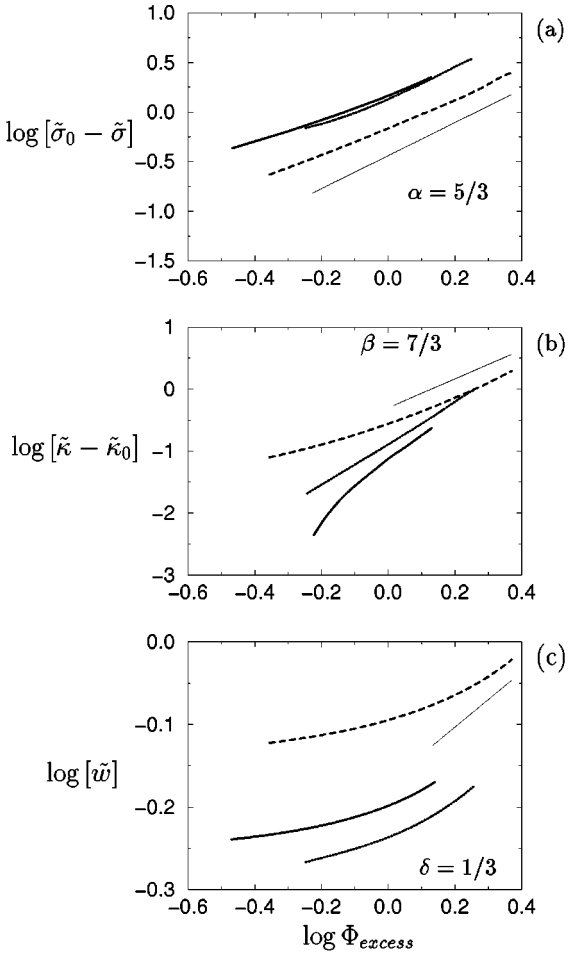

FIG. 12. Log-log plots of (a) the surface pressure $(\tilde{\sigma}_0-\tilde{\sigma})$, (b) excess in the bending rigidity, and (c) the width of the excess copolymer layer at the interface as a function of the excess amount of copolymers at the interface, Φ_{excess}. The solid lines correspond to $\gamma=1$ and $\chi N=12$; the dotted lines correspond to $\gamma=1$ and $\chi N=20$; and the dashed lines correspond to $\gamma=2$ and $\chi N=12$. The thin solid lines indicates the slopes predicted by the scaling arguments for wet polymer brushes.

IV. CONCLUSION

In this paper, we have presented a theory of Gaussian fluctuations in the semi-grand canonical ensemble, on top of the self-consistent mean field theory, for a ternary mixture consisting of two homopolymers and diblock copolymers. The theory enables us to obtain the two-point correlation function of the volume fraction fluctuations, from which the power spectrum of the interfacial capillary modes is derived. The availability of the power spectrum allows us to calculate the interfacial tension and the bending rigidity of the interface. In particular, we found that the values of the surface tension as calculated from our method are consistent with those calculated from the excess free energy within the self-consistent field theory.

In the limiting case of a pure binary homopolymer mixture, we found that while the interfacial tension increases with increasing χN, the bending rigidity exhibits a non-monotonic behavior; namely it increases with χN in the neighborhood of the critical point, but then decreases with further increase of χN. Our results were explained using the self-consistent field calculations of Helfand and Nagami[30] and scaling arguments.

In the presence of diblock copolymers, the interfacial tension always decreases with increasing the volume fraction of the diblock copolymers. However, the bending rigidity may either decrease with increasing ϕ^c_{bulk} for high temperatures (low χN), or increase for low temperatures or/and high molecular weight of the copolymers. Finally, we have also qualitatively compared our results for the surface pressure induced by the aggregated copolymers at the interface, the excess bending rigidity and the copolymer interfacial layer, with the scaling arguments of Leibler in the limiting case of wet polymer brushes. In particular, we found that whereas no agreement is observed for low volume fractions of the diblock copolymers, a fairly good agreement, especially for the interfacial tension and the interfacial width, is observed when the triple line is approached. The agreement also improves with increasing χN and the relative diblock copolymer molecular weight.

Finally, it is useful to mention that our study of block

copolymers at interfaces is also motivated by the fact that these systems can well be regarded as a theoretical model for the more complex biological systems corresponding to lipid membranes which are decorated by homopolymers very often contain proteins which are coupled to a polymer brush known as the *glycocalyx*.[31] In order to understand these complex systems, simplified experimental models consisting of membranes made of phospholipids which are chemically attached to poly(ethylene glycol), are used.[32] In particular, it is observed that the grafted polymer chains alter drastically the elastic properties of the lipid bilayer. Liposomes containing homopolymer-grafted lipids are also being used for *in vivo* drug delivery. In fact, due to their long circulation time scales in blood as compared to that of bare liposomes, polymer-decorated liposomes can be directed to very specific targets in the body.[33]

ACKNOWLEDGMENT

This work was supported by the Natural Sciences and Engineering Research Council of Canada.

APPENDIX A: MEAN FIELD PHASE DIAGRAM

In this appendix, we show how the phase diagram is determined assuming that the ternary system can be found only in homogeneous states, corresponding to the A-rich, B-rich and disordered phases. For such calculation, it is useful to introduce the end-integrated propagators,

$$q_\alpha(\mathbf{r},t)=\int d\mathbf{r}'\,Q_\alpha^{(0)}(\mathbf{r},t|\mathbf{r}'), \tag{A1}$$

$$q_{\mathrm{A}}^c(\mathbf{r},t)=\int d\mathbf{r}'\,d\mathbf{r}''\,Q_{\mathrm{A}}^{(0)}(\mathbf{r},t|\mathbf{r}')Q_{\mathrm{B}}^{(0)}\left(\mathbf{r}',\frac{\gamma}{2}\middle|\mathbf{r}''\right), \tag{A2}$$

$$q_{\mathrm{B}}^c(\mathbf{r},t)=\int d\mathbf{r}'\,d\mathbf{r}''\,Q_{\mathrm{B}}^{(0)}(\mathbf{r},t|\mathbf{r}')Q_{\mathrm{A}}^{(0)}\left(\mathbf{r}',\frac{\gamma}{2}\middle|\mathbf{r}''\right), \tag{A3}$$

which, using Eq. (12), are shown to satisfy the following modified diffusion equations

$$\frac{\partial}{\partial t}q_\alpha(\mathbf{r},t)=\nabla^2 q_\alpha(\mathbf{r},t)-\omega_\alpha^{(0)}(\mathbf{r})q_\alpha(\mathbf{r},t), \tag{A4}$$

$$\frac{\partial}{\partial t}q_\alpha^c(\mathbf{r},t)=\nabla^2 q_\alpha^c(\mathbf{r},t)-\omega_\alpha^{(0)}(\mathbf{r})q_\alpha^c(\mathbf{r},t), \tag{A5}$$

with the boundary conditions

$$q_{\mathrm{A}}(\mathbf{r},0)=1, \tag{A6}$$

$$q_{\mathrm{B}}(\mathbf{r},0)=1, \tag{A7}$$

$$q_{\mathrm{A}}^c(\mathbf{r},0)=q_{\mathrm{B}}\left(\mathbf{r},\frac{\gamma}{2}\right), \tag{A8}$$

$$q_{\mathrm{B}}^c(\mathbf{r},0)=q_{\mathrm{A}}\left(\mathbf{r},\frac{\gamma}{2}\right). \tag{A9}$$

Using Eqs. (20)–(23), we find that the mean field volume fractions are given by

$$\phi_{\mathrm{A}}^{h(0)}(\mathbf{r})=\int_0^1 dt\,q_{\mathrm{A}}(\mathbf{r},t)q_{\mathrm{A}}(\mathbf{r},1-t), \tag{A10}$$

$$\phi_{\mathrm{B}}^{h(0)}(\mathbf{r})=\int_0^1 dt\,q_{\mathrm{B}}(\mathbf{r},t)q_{\mathrm{B}}(\mathbf{r},1-t), \tag{A11}$$

$$\phi_A^{c(0)}(\mathbf{r})=e^{\mu_c}\int_0^{\frac{\gamma}{2}} dt\,q_{\mathrm{A}}(\mathbf{r},t)q_{\mathrm{A}}^c\left(\mathbf{r},\frac{\gamma}{2}-t\right), \tag{A12}$$

$$\phi_{\mathrm{B}}^{c(0)}(\mathbf{r})=e^{\mu_c}\int_0^{\frac{\gamma}{2}} dt\,q_{\mathrm{B}}(\mathbf{r},t)q_{\mathrm{B}}^c\left(\mathbf{r},\frac{\gamma}{2}-t\right). \tag{A13}$$

For spatially homogeneous phases, the end-integrated propagators are independent of $\mathbf{r}$, $q_\alpha(\mathbf{r},t)\equiv q_\alpha(t)$ and $q_\alpha^c(\mathbf{r},t)\equiv q_\alpha^c(t)$. These are found to be

$$q_\alpha(t)=e^{-\omega_\alpha^{(0)}t}, \tag{A14}$$

$$q_{\mathrm{A}}^c(t)=e^{-\omega_{\mathrm{A}}^{(0)}t-\omega_{\mathrm{B}}\frac{\gamma}{2}}, \tag{A15}$$

$$q_{\mathrm{B}}^c(t)=e^{-\omega_{\mathrm{B}}^{(0)}t-\omega_{\mathrm{A}}\frac{\gamma}{2}}, \tag{A16}$$

and the volume fractions are then calculated using Eqs. (A10)–(A13):

$$\phi_{\mathrm{A}}^{h(0)}=e^{-\omega_{\mathrm{A}}^{(0)}}, \tag{A17}$$

$$\phi_{\mathrm{B}}^{h(0)}=e^{-\omega_{\mathrm{B}}^{(0)}}, \tag{A18}$$

$$\phi_{\mathrm{A}}^{c(0)}=\phi_{\mathrm{B}}^{c(0)}=\frac{\gamma}{2}e^{\mu_c}e^{-\frac{\gamma}{2}(\omega_{\mathrm{A}}^{(0)}+\omega_{\mathrm{B}}^{(0)})}. \tag{A19}$$

Using the fact that auxiliary fields and the volume fractions are also related by the mean field equations, Eqs. (18) and (19), one finds the order parameter ψ of the homogeneous phases,

$$\psi=(\phi_{\mathrm{A}}^{h(0)}+\phi_{\mathrm{A}}^{c(0)})-(\phi_{\mathrm{B}}^{h(0)}+\phi_{\mathrm{B}}^{c(0)}) \tag{A20}$$

and the diblock copolymer volume fraction $\phi_{\mathrm{bulk}}^c\equiv\phi_A^{c(0)}+\phi_B^{c(0)}$ satisfy the following equations,

$$1-\psi\coth\left(\frac{\chi N}{2}\psi\right)=\gamma 2^\gamma e^{\mu_c}\psi^\gamma\left[\coth^2\left(\frac{\chi N}{2}\psi\right)-1\right]^{\frac{\gamma}{2}} \tag{A21}$$

and

$$\phi_{\mathrm{bulk}}^c=1-\psi\coth\left(\frac{\chi N}{2}\psi\right), \tag{A22}$$

respectively. The phase diagram is then calculated by comparing the free energy densities of homogeneous phases given by

$$f_{\mathrm{hom}}=\frac{\chi N}{4}(1-\psi^2)+\left(\frac{1+\psi}{2}\right)\ln\left(\frac{1-\phi_{\mathrm{bulk}}^c+\psi}{2}\right)+\left(\frac{1-\psi}{2}\right)\ln\left(\frac{1-\phi_{\mathrm{bulk}}^c-\psi}{2}\right)+\left(1-\frac{1}{\gamma}\right)\phi_{\mathrm{bulk}}^c. \tag{A23}$$

APPENDIX B: NUMERICAL SELF-CONSISTENT FIELD THEORY

The basic equations for calculating the mean field profile in the two phase region of the phase diagram are Eqs. (A1)–

(A9). In order to determine the interfacial profile, we consider a system of linear size L in the z direction. We first calculate the values of volume fractions at two-phase coexistence from the bulk free energy density (see Appendix A), and we fix the interface to be at $z=0$. We moreover assume that the system is homogeneous along the $x-y$ plane. The values of homopolymer volume fraction is chosen to have different equilibrium coexistence values; namely ϕ_{A}^{h} and ϕ_{B}^{h} assumes the value of the homopolymer volume fractions of the A-rich phase at $z=-L/2$ and that of the B-rich phase at $z=L/2$.

The numerical method for determining the volume fraction profile is as follows:

(1) At a certain point of the parameter space $(\mu_c,\chi N,\gamma)$, we determine $\phi_{\alpha}^{h(0)}$ and $\phi_{\alpha}^{c(0)}$ corresponding to the two-phase region.
(2) We make an initial guess for $\omega_{\mathrm{A}}^{(0)}(z)$ and $\omega_{\mathrm{B}}^{(0)}(z)$. Their values at $z=\pm L/2$ are calculated according to Eqs. (A14) and (A15). We further set $\omega_{\alpha}^{(0)}(z<0)=\omega_{\alpha}^{(0)}(-L/2)$, $\omega_{\alpha}^{(0)}(z>0)=\omega_{\alpha}^{(0)}(L/2)$, and $\omega_{\alpha}^{(0)}(0)=[\omega_{\alpha}^{(0)}(-L/2)+\omega_{\alpha}^{(0)}(L/2)]/2$.
(3) We solve the modified diffusion equation for the end-integrated propagators, Eqs. (A4) and (A5), with the appropriate boundary conditions using the potentials $\omega_{A}^{(0)}\times(z)$ and $\omega_{\mathrm{B}}^{(0)}(z)$. These propagators are then used to evaluate the volume fractions, $\phi_{\alpha}^{h(0)}$ and $\phi_{\alpha}^{c(0)}$ using Eqs. (A10)–(A13). Notice that in general, the incompressibility condition will not be met.
(4) The local Lagrange multiplier, $\eta(z)$ is calculated from combining Eqs. (18), (19) and (24), i.e.,

$$\eta(z)=\frac{1}{2}[\omega_{\mathrm{A}}^{(0)}(z)+\omega_{\mathrm{B}}^{(0)}]. \tag{B1}$$

(5) Using the new values for the volume fractions and Lagrange multipliers, we calculate

$$\delta\omega_{\mathrm{A}}^{(0)}(z)=\chi N[\phi_{\mathrm{B}}^{h(0)}(z)+\phi_{\mathrm{B}}^{c(0)}(z)]+\eta(z)-\omega_{\mathrm{A}}^{(0)}(z), \tag{B2}$$

$$\delta\omega_{\mathrm{B}}^{(0)}(z)=\chi N[\phi_{\mathrm{A}}^{h(0)}(z)+\phi_{\mathrm{A}}^{c(0)}(z)]+\eta(z)-\omega_{\mathrm{B}}^{(0)}(z), \tag{B3}$$

$$\delta\phi(z)=1-\sum_{\alpha}[\phi_{\alpha}^{h(0)}(z)+\phi_{\alpha}^{c(0)}(z)]. \tag{B4}$$

The iteration is stopped if the values of $|\delta\omega_A(z)|$ and $|\delta\omega_B(z)|$ and $|\delta\phi(z)|$ are smaller than a certain convergence criterion (we typically take 10^{-7}). Otherwise, we calculate the new values for the auxiliary fields:

$$\omega_{\alpha}^{\mathrm{new}}(z)=\omega_{\alpha}(z)+\rho\,\delta\omega_{\alpha}(z)-\beta\,\delta\phi(z), \tag{B5}$$

where ρ and β are small positive numbers (we typically use $\beta=\rho=0.1$) and we return with the new guesses for $\omega_{\alpha}^{\mathrm{new}}$ to step 3.

The modified diffusion equations are integrated using the Crank-Nicholson method with an arc-length mesh typically equal to $\Delta t=1/200$ and a mesh-size Δz varying from 0.05 to 0.1.

[1] F. S. Bates, W. W. Maurer, P. M. Lipic, M. A. Hillmyer, K. Almdal, K. Mortensen, G. H. Fredrickson, and T. P. Lodge, Phys. Rev. Lett. **79**, 849 (1997).
[2] R. A. L. Jones, E. J. Kramer, M. H. Rafailovich, and S. A. Schwarz, Phys. Rev. Lett. **62**, 280 (1989).
[3] K. R. Shull, E. J. Kramer, G. Hadziioannou, and W. Tang, Macromolecules **23**, 4780 (1990).
[4] K. H. Dai, E. J. Kramer, and K. R. Shull, Macromolecules **25**, 220 (1992).
[5] K. H. Dai, L. J. Norton, and E. J. Kramer, Macromolecules **26**, 1949 (1994).
[6] K. R. Shull, A. M. Mayes, and T. P. Russell, Macromolecules **26**, 3929 (1993).
[7] W. Hu, J. T. Koberstein, J. P. Lingelser, and Y. Gallot, Macromolecules **28**, 5209 (1995).
[8] E. Helfand, Macromolecules **8**, 552 (1975).
[9] K. M. Hong and J. Noolandi, Macromolecules **14**, 727 (1981); **14**, 736 (1981).
[10] J. Noolandi and K. M. Hong, Macromolecules **15**, 482 (1982).
[11] J. Noolandi and K. M. Hong, Macromolecules **17**, 1531 (1984).
[12] T. A. Vilgis and J. Noolandi, Makromol. Chem., Macromol. Symp. **16**, 225 (1988).
[13] L. Leibler, Makromol. Chem., Macromol. Symp. **16**, 1 (1988).
[14] K. R. Shull and E. J. Kramer, Macromolecules **23**, 4769 (1990).
[15] M. W. Matsen, Phys. Rev. Lett. **74**, 4225 (1995).
[16] J. Noolandi, Makromol. Chem. **12**, 517 (1991).
[17] Z.-G. Wang and S. A. Safran, J. Chem. Phys. **94**, 679 (1991); J. Phys. (France) **51**, 185 (1990).
[18] M. W. Matsen and M. Schick, Macromolecules **26**, 3873 (1993); **27**, 2316 (1994).
[19] M. Müller and M. Schick, J. Chem. Phys. **105**, 8885 (1996).
[20] A. Werner, F. Schmid, K. Binder, and M. Müller, Macromolecules **29**, 8241 (1996).
[21] L. Leibler, Macromolecules **13**, 1602 (1980); **15**, 1283 (1982).
[22] C. Yeung, A.-C. Shi, R. C. Desai, and J. Noolandi, Macromol. Theory Simul. **5**, 291 (1996).
[23] A.-C. Shi, J. Noolandi, and R. C. Desai, Macromolecules **29**, 6487 (1996).
[24] M. Laradji, A.-C. Shi, R. C. Desai, and J. Noolandi, Phys. Rev. Lett. **78**, 2577 (1997).
[25] M. Laradji, A.-C. Shi, J. Noolandi, and R. C. Desai, Macromolecules **30**, 3242 (1997).
[26] E. Helfand, J. Chem. Phys. **62**, 999 (1975).
[27] P. K. Jannert and M. Schick, Macromolecules **30**, 137 (1997); **30**, 3916 (1997).
[28] M. W. Matsen and M. Schick, Phys. Rev. Lett. **72**, 2660 (1994).
[29] C. Yeung, R. C. Desai, and J. Noolandi, Macromolecules **27**, 55 (1993).
[30] E. Helfand and Y. Tagami, J. Chem. Phys. **56**, 3592 (1972).
[31] *Structure and Dynamics of Membranes*, edited by R. Lipowsky and E. Sackmann (Elsevier, Amsterdam, 1995), Vol. 1.
[32] G. Blume and G. Cevc, Biochim. Biophys. Acta **1029**, 91 (1990).
[33] D. Lasic, Angew. Chem. Int. Ed. Engl. **33**, 1685 (1994).